

## Phase Diagrams for Staged Intercalation Compounds

S. A. Safran

*Bell Laboratories, Murray Hill, New Jersey 07974*

(Received 4 December 1979)

The phase diagram for a staged intercalation compound is calculated in mean-field theory. At low temperatures, the dependence of the staging on the chemical potential is related to the interlayer interactions responsible for staging. At high temperatures, a dilute stage-1 phase is predicted for all values of the chemical potential. The stage-2-stage-1 transition is second order for temperatures greater than the tricritical temperature. The predicted phase diagrams are related to recent experiments.

PACS numbers: 61.60.+m, 64.60.Cn, 64.70.Kb

One of the most interesting, but poorly understood phenomena observed in intercalation compounds is the existence of pure stage ordering—a periodic sequence of  $n$  host layers and one intercalant layer. Although the best examples of staging have been observed in graphite intercalation compounds,<sup>1,2</sup> where high stages ( $n \sim 10$ ) have been prepared, certain intercalation compounds of the transition-metal dichalcogenides have been shown to stage as well.<sup>3</sup> In this paper, the simplest possible, physically reasonable Hamiltonian that shows staging is treated to yield phase diagrams as functions of chemical potential, temperature, and concentration. The mean-field theory of staging is preceded by an exact, numerical study at zero temperature of a one-dimensional Ising model with long-range interactions in an external field (chemical potential). Although there is also current interest in magnetic systems with one-dimensional modulated structures,<sup>4-6</sup> the present study focuses on the application to intercalation compounds. The main new results of this work are the predictions of a limiting temperature  $T_m$  above which only stage 1 is stable and of a second-order phase transition from stage 2 to stage 1 in a limited region of the phase diagram.

The model Hamiltonian used in the present calculations consists of attractive in-plane interactions and repulsive interplanar interactions between intercalants. A mean-field approximation is then used to treat the in-plane interactions, so that the Hamiltonian becomes, after the in-plane averaging,

$$H = -\mu \sum_i \sigma_i - \frac{1}{2} U_0 \sum_i \sigma_i^2 + \frac{1}{2} \sum_{ij} V_{ij} \sigma_i \sigma_j. \quad (1)$$

In Eq. (1)  $i$  is a layer index and  $U_0 > 0$  and  $V_{ij} > 0$  are, respectively, the averaged in-plane and interplanar interaction energies;  $\mu$  is the chemical potential while the  $\{\sigma_i\}$  are the average layer oc-

cupancies of the intercalant sites, which may take continuous values between 0 and 1. Since this work deals with the case of weak interlayer repulsion in comparison with the in-plane attraction, the assumption of a homogeneous concentration of intercalant within the plane is justified within mean-field theory. In addition, since stage ordering exists in a wide variety of graphite intercalation compounds with different forms of in-plane order<sup>7-10</sup> (commensurable/incommensurable with host) or disorder<sup>8-10</sup> (lattice-gas-like, liquidlike), the exact nature of the in-plane structure does not seem to be crucial. Thus, the intercalant planes are characterized by their (temperature-dependent) average densities only. The interplanar repulsion is modeled as a power law  $V_{ij} = \frac{1}{2} V |z_{ij}|^{-\alpha}$ , where  $|z_{ij}|$  is the distance between planes  $i$  and  $j$ , measured in units of the  $c$ -axis lattice spacing. Although a detailed analysis of the microscopic origin of the interplanar repulsive interactions is beyond the scope of this paper, it may be noted that the screening of the intercalant layer in graphite intercalation compounds follows a power law<sup>11</sup> (and not an exponential one). Thus, the electrostatic repulsions of the intercalant layers, which have donated their electrons to the host, could be the origin of the long-range interaction responsible for stage ordering.<sup>12</sup> Moreover, as shown below, the repulsive power-law interaction does produce staging, so it is useful to study the Hamiltonian (1) as a model system with  $V$  and  $\alpha$  treated as phenomenological parameters.

At  $T = 0$ , the layer occupancies  $\{\sigma_i\}$  were assumed to be periodic functions<sup>4</sup> and a numerical calculation was used to find the configuration which minimized the total energy for each value of  $\mu$ . For computational convenience, a cutoff  $\tilde{z}$  was introduced in  $V_{ij}$  so that the maximum periodicity investigated was  $\tilde{z}$  ( $\tilde{z} = 15$  for the  $T = 0$  cal-

ulation). The results of this calculation are shown in Table I where the ranges of stability,  $\Delta\tilde{\mu}(\tilde{n})$ , are listed. Here,  $\tilde{n}$ , which is the inverse of the average concentration, takes on integer values for pure stage ordering. The range of stability is the range of  $\mu$  values over which a given phase is stable and  $\tilde{\mu} \equiv (\mu + \frac{1}{2}U_0)/\tilde{V}$ , where  $\tilde{V} = V\xi(\alpha)$  and  $\xi(\alpha) = \sum_{p=1}^{\infty} p^{-\alpha}$  for the cutoff  $\tilde{z} \rightarrow \infty$ . In terms of the variable  $\tilde{\mu}$ , we have  $\tilde{n}^{-1} = 0$  for  $\tilde{\mu} < 0$  and  $\tilde{n} = 1$  for  $\tilde{\mu} > 1$ . As shown in Table I, more and more of the phase diagram at  $T = 0$  is dominated by the pure stages for increasing  $\alpha$  a large number of high-order commensurate nonpure-stage ( $\tilde{n}$  nonintegral) configurations<sup>13, 14</sup> are obtained at  $T = 0$ . On the other hand, for  $\alpha = 4$  the range of stability of the nonpure stages is at least an order of magnitude less than that of the pure stages! The  $T = 0$  ranges of stability for pure stages are shown in Fig. 1.

For a model containing only pure stages,<sup>12</sup> it can be shown that, at  $T = 0$ ,

$$\Delta\mu(n) = n |g(n+1) + g(n-1) - 2g(n)|, \quad (2)$$

where  $g(n) = \sum_{p=1}^{\infty} V_{t, t+pn}$ . For the power-law interaction considered here, Eq. (2) agrees with the numerical results of Table I for  $\alpha = 4$  where the nonpure stages are negligible for  $\tilde{n} > 2$ . Thus, the experimentally determined, low temperature, range of stability as a function of stage yields directly the stage dependence of the interlayer in-

TABLE I. Ranges of stability of  $T = 0$  phases.  $\tilde{n}$  is the inverse of the average concentration;  $\Delta\tilde{\mu}$  is the range of stability, and  $\alpha$  characterizes the power-law interaction defined in the text.  $\tilde{n} = n$  (an integer) represents pure-stage ordering. The range of stability for  $\tilde{n}$  nonintegral consists of the sum of the ranges of stability for all nonpure stages with concentrations in the indicated range.

Inverse average concentration	$\Delta\tilde{\mu} (\alpha = 2)$	$\Delta\tilde{\mu} (\alpha = 4)$
$\tilde{n} > 5$	0.0571	0.0030
$\tilde{n} = 5$	0.0074	0.0035
$4 < \tilde{n} < 5$	0.0042	0.0002
$\tilde{n} = 4$	0.0511	0.0118
$3 < \tilde{n} < 4$	0.0203	0.0009
$\tilde{n} = 3$	0.0847	0.0592
$2 < \tilde{n} < 3$	0.0532	0.0050
$\tilde{n} = 2$	0.4470	0.8339
$1 < \tilde{n} < 2$	0.2750	0.0825

teractions responsible for staging. Although the variation in  $\mu$  in going from one stage to the next is quite small, such changes can be controlled experimentally since the chemical potential is a logarithmic function of the equilibrium vapor pressure. It may be noted that within the present model there is always a region of nonpure stages<sup>14</sup> for  $1 < \tilde{n} < 2$ , related to the region of pure stages for  $\tilde{n} > 2$  by the symmetry (empty/filled) about  $\tilde{n} = 2$  implied by binary interactions. However, since there is as yet no experimental evidence for such states (e.g., three layers filled, one empty for  $\tilde{n} = \frac{4}{3}$ ) it is not clear that the model of concentration-independent interactions<sup>12</sup> is appropriate for intercalant densities near saturation. Careful *in situ* x-ray experiments have yet to be performed in this region.

The phase diagram in the  $(\mu, T)$  and  $(\tilde{n}, T)$  planes was calculated in mean-field theory, assuming that the nonpure stages, which occupy a small portion of the  $T = 0$  phase diagram, are negligible for  $T > 0$  as well.<sup>12</sup> Since there is no interaction between configurations within mean-field theory, the presence of nonpure stages in a small region of phase space would not affect the validity of the calculation for the pure stages. Periodicities up to a maximum of  $n = 10$  were investigated and the mean-field free energy was calculated using the

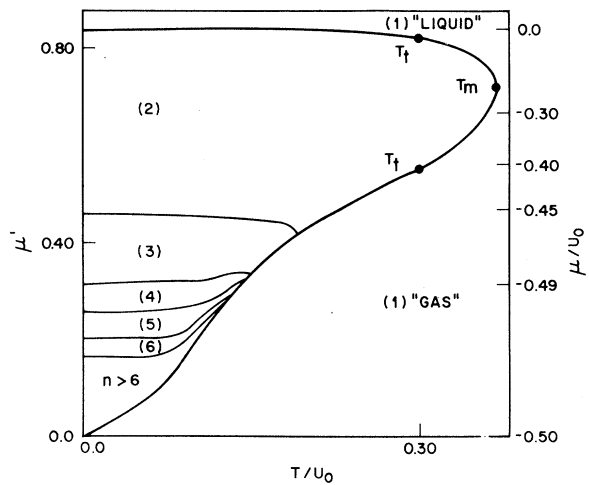


FIG. 1. Phase diagram for  $V = \frac{1}{2}U_0$  and  $\alpha = 4$  plotted as a function of temperature  $T$  and chemical potential  $\mu$ , both normalized to  $U_0$ . For clarity, the phase diagram is given as a linear function of  $\mu' = (\mu/U_0 + \frac{1}{2})^{1/\alpha}$ —leading to a nonlinear  $\mu$  scale on the right-hand side of the figure. The integers in parentheses are the stable pure-stage phases.  $T_m$  and  $T_t$  are the maximum and tricritical temperatures, respectively.

relation<sup>15</sup>

$$\sigma_i = \left\{ \exp[\beta(-\mu - U_0\sigma_i + \sum_j V_{ij}\sigma_j)] + 1 \right\}^{-1}, \quad (3)$$

where  $\beta = 1/kT$ . The mean-field equations were solved self-consistently for  $n = 1, 2$ , and 3, while for  $n = 4, \dots, 10$  a low-temperature expansion was used. This expansion is justified by the fact that these stages are only stable at low temperatures where the variations in the concentration are small.

The resulting phase diagrams are shown in Figs. 1 and 2 for an interlayer interaction with  $\alpha = 4$  and  $V = \frac{1}{2}U_0$ . As shown in Fig. 1, the high-stage phases all terminate in a dilute stage-1 phase ("gas") whose concentration goes to zero as  $T \rightarrow 0$ . The transitions from stage to stage for  $n > 2$  are all of first order for a model with weak interlayer interactions and the concentration ranges over which these states are stable are within 6% of their  $T = 0$  concentrations as shown in Fig. 2. On the other hand, the stage-2–stage-1 transition is second order for  $T > T_t$ , with a large range of stoichiometries predicted for the stage-2 phase at high temperatures as shown in Fig. 2. Furthermore, since the stage-2–stage-1 transition is isomorphic to that of a metamagnet in a magnetic field,<sup>16, 17</sup> the maximum temperature at which stage two is stable is given by

$$T_m = \frac{1}{4}(U_0 - V_a + V_b), \quad (4)$$

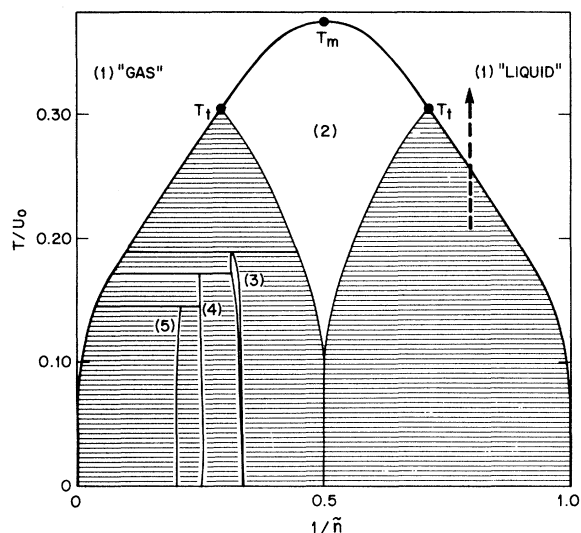


FIG. 2. Same phase diagram as in Fig. 1 plotted as a function of normalized temperature  $T/U_0$  and concentration  $n^{-1}$ . The integers in parentheses are the single-phase pure-stage states, while the cross-hatched areas denote two-phase regions. For clarity only stages 1 through 5 have been shown.

while the tricritical point ( $T_t$ ) is given by

$$T_t/T_m = 1 - V_b/[3(U_0 - V_a)]. \quad (5)$$

Here,  $V_a = V2^{-\alpha}\xi(\alpha)$  while  $V_a + V_b = V\xi(\alpha)$ . With the values for  $V$  and  $\alpha$  given above, this yields  $T_m = 0.37U_0$  and  $T_t = 0.30U_0$  in agreement with the numerical calculations of Fig. 1. For  $T < T_m$  the stage-1 phase is divided into "gas" and "liquid" phases, each having a restricted range of composition, while for  $T > T_m$  the composition range is unrestricted and no staged ( $n > 1$ ) states are stable. The cross-hatched areas in Fig. 2 represent states in a two-phase region.

In Fig. 2, the symmetry of the outermost phase boundary about  $\tilde{n}^{-1} = \frac{1}{2}$  is due to the simple model of two-body attractive in-plane interactions. More complicated (and realistic) representations of the in-plane interactions would result in a less-symmetric phase boundary. Although the exact nature of the in-plane ordering is not addressed by the mean-field theory, it must be noted that all changes of stage as a function of temperature (Figs. 1 and 2) occur because of changes in the average in-plane density [Eq. (3)]. For example, the continuous stage-2–stage-1 transition at  $T = T_m$  can be understood as arising from a density distribution of  $(\sigma_1, \sigma_2) = (1, 0)$  at  $T = 0$ . As the temperature is increased, "vacancies" are created in layer 1 and "interstitials" in layer 2 so that at  $T = T_m$ ,  $(\sigma_1, \sigma_2) = (\frac{1}{2}, \frac{1}{2})$ —a state which is indistinguishable from a dilute stage 1.

Although no systematic *in situ* x-ray studies of the equilibrium phase diagrams of intercalation compounds have as yet been reported, recent x-ray measurements of in-plane densities of graphite intercalation compounds<sup>18</sup> have shown departures from the ideal low-temperature stoichiometries. In addition, the transition from stage 1 to a two-phase stage-1–stage-2 mixture at fixed concentration ( $\tilde{n}^{-1} = 0.8$  as shown by the dashed line in Fig. 2 has been reported to occur at  $T_0 \approx 600$  K for Cs-graphite intercalation compounds.<sup>10</sup> Figure 2 indicates that  $T_0/U_0 = 0.24$ , so that  $U_0 \approx 2400$  K and  $T_m \approx 925$  K for the Cs-graphite system. Future experiments can test the simple model presented here by first looking for the dilute "gas" stage-1 phase. Secondly, after searching for the existence of nonpure stages,<sup>14</sup> the temperature and chemical-potential dependence of the stage-2 concentration should be checked to confirm the existence of  $T_t$  and  $T_m$ . Finally, the ranges of stability of the high-stage compounds should be investigated since they are directly related to the form of the repulsive interlayer inter-

action. Such experimental information would facilitate further elaboration of the simple theory described here, such as the introduction of many-body interactions or couplings to other (elastic, electronic) degrees of freedom.

The author is grateful to P. C. Hohenberg for his interest and suggestions. Useful discussions with M. C. Cross, F. J. Di Salvo, D. S. Fisher, M. E. Fisher, and D. R. Hamann are also acknowledged.

<sup>1</sup>For general reviews, see J. E. Fischer and T. E. Thompson, *Phys. Today* **31**, No. 7, 36 (1978), and *Mater. Sci. Eng.* **31**, 1977.

<sup>2</sup>Proceedings of the International Conference on Layered Materials and Intercalates, Nijmegen, The Netherlands, 1979 [*Physica (Utrecht)* **99B**, (1980)].

<sup>3</sup>H. Fernandez-Moran, M. Ohstuki, A. Hibino, and C. Hough, *Science* **174**, 498 (1971); A. Soreau, M. Danot, L. Trichet, and J. Rouxel, *Mater. Res. Bull.* **9**, 191 (1974).

<sup>4</sup>J. von Boehm and P. Bak, *Phys. Rev. Lett.* **42**, 122 (1978).

<sup>5</sup>P. Bak and J. von Boehm, *Phys. Rev. B* (to be published).

<sup>6</sup>W. Selke and M. E. Fisher, *Phys. Rev. B* **20**, 257 (1979).

<sup>7</sup>N. Kambe, M. S. Dresselhaus, G. Dresselhaus, S. Basu, A. R. McGhie, and J. E. Fischer, *Mater. Sci. Eng.* **40**, 1 (1979).

<sup>8</sup>See the papers by H. Zabel, Y. M. Jan, and S. C.

Moss, *Physica (Utrecht)* **99B**, 453 (1980); R. Clarke, N. Caswell, S. A. Solin, and P. M. Horn, *Physica (Utrecht)* **99B**, 457 (1980).

<sup>9</sup>N. Caswell, S. A. Solin, T. M. Hayes, and S. J. Hunter, *Physica (Utrecht)* **99B**, 463 (1980).

<sup>10</sup>R. Clarke, N. Caswell, and S. A. Solin, *Phys. Rev. Lett.* **42**, 61 (1979).

<sup>11</sup>L. Pietronero, S. Strässler, H. R. Zeller, and M. J. Rice, *Phys. Rev. Lett.* **41**, 763 (1978).

<sup>12</sup>S. A. Safran and D. R. Hamann, *Physica (Utrecht)* **99B**, 469 (1980), and to be published. In the work to be published, nonlinear electrostatic screening is shown to lead to *pure* stage ordering in graphite intercalation compounds (i.e., nonpure stages are excluded).

<sup>13</sup>This is in contrast to the behavior reported in the model studied in Refs. 4–6. In the present work, the competition is between the external field (chemical potential) and the interactions. References 4–6 examined a model in zero field with competing interactions. We note that for  $\alpha \geq 2$ , the case considered here, the first- and second-neighbor interactions are no longer competing.

<sup>14</sup>In this work, “*nonpure* stage” refers to a *single-phase*, ordered, periodic sequence of layers (e.g., three empty, one filled, two empty, one filled...) and not to a *mixed* phase of pure stages.

<sup>15</sup>A. G. Khachatryan, *Phys. Status Solidi (b)* **60**, 9 (1973).

<sup>16</sup>D. Furman and M. Blume, *Phys. Rev. B* **10**, 2068 (1974).

<sup>17</sup>J. M. Kincaid and E. G. D. Cohen, *Phys. Rep. C* **22**, 75 (1975).

<sup>18</sup>S. Y. Leung, C. Underhill, G. Dresselhaus, T. Krapchev, R. Ogilvie, and M. S. Dresselhaus, *Solid State Commun.* **32**, 635 (1979).

## Computer Simulation of Crack Propagation

Arthur Paskin and A. Gohar

*Queens College of the City University of New York, Flushing, New York 11367*

and

G. J. Dienes

*Brookhaven National Laboratory, Upton, New York 11973*

(Received 25 January 1980)

Computer simulations of crack properties were performed on a two-dimensional triangular lattice with a Lennard-Jones interatomic interaction. The use of a long-range potential and an unconstrained sample revealed novel features compared to earlier simulations. The Griffith energy treatment for fracture was found wanting. This system is brittle at low stresses in agreement with the Rice-Thomson criterion and shows dislocation formation at elevated stresses.

Brittle fracture is an important material property and yet has received relatively little attention with respect to the underlying atomic mechanisms. Indeed, it is only with the advent of modern computers that dynamic investigations be-

came possible.<sup>1-3</sup> Prior to these recent developments essentially all approaches were based on continuum mechanics,<sup>4</sup> and elastic statics.<sup>5</sup> Griffith has shown how energy criteria and continuum mechanics can be combined to yield a critical